Predicting the Effects of Test Media in Ground-Based Propulsion Testing

J. Philip Drummond[*] , Paul M. Danehy[†] , Daniel Bivolaru[‡] ,
Richard L. Gaffney[§] and Peter A. Parker[¶]
NASA Langley Research Center, Hampton, VA

Harsha K. Chelliah[‖]
University of Virginia, Charlottesville, VA

Andrew D. Cutler[**]
The George Washington University, Hampton, VA

Peyman Givi[††]
University of Pittsburgh, Pittsburgh, PA

Hassan A. Hassan[‡‡]
North Carolina State University, Rayleigh, NC

Abstract

[*]Hypersonic Air Breathing Propulsion Branch

[†]Advanced Sensing and Optical Measurements Branch

[‡]NASA Post-Doctoral Fellow

[§]Hypersonic Air Breathing Propulsion Branch

[¶]Aeronautics Systems Engineering Branch

[‖]Associate Professor, Department of Mechanical and Aerospace Engineering

[**]Professor, Department of Aerospace Engineering

[††]William Kepler Whiteford Professor of Engineering, Department of Mechanical Engineering

[‡‡]Professor, Department of Aerospace Engineering

This paper discusses the progress of work which began in mid-2004 sponsored by the Office of the Secretary of Defense (OSD) Test & Evaluation/Science & Technology (T&E/S&T) Program. The purpose of the work is to improve the state of the art of CFD capabilities for predicting the effects of the test media on the flameholding characteristics in scramjet engines. The program has several components including the development of advance algorithms and models for simulating engine flowpaths as well as a fundamental experimental and diagnostic development effort to support the formulation and validation of the mathematical models. The paper will provide details of current work in-

1

volving the development of phenomenological models for Reynolds averaged Navier-Stokes codes, large-eddy simulation techniques and reduced-kinetics models. Experiments that will provide data for the modeling efforts will also be described, along with with the associated nonintrusive diagnostics used to collect the data.

Introduction

The design and development of a scramjet engine is accomplished with several levels of analytic tools, ground-based testing and finally flight. To achieve the flight conditions encountered by a scramjet propelled hypersonic vehicle in a ground facility, the test gas must be heated to high temperatures before being introduced into the engine flowpath. One method for heating the test gas involves mixing fuel, for example hydrogen or butane, with the air and allowing it to combust in a facility heater prior to use. After the fuel is burned, oxygen is added to the test gas to make up for the oxygen depleted during combustion. As a consequence of chemical reaction, combustion products, or vitiates, are also added to the test gas. These products can affect the performance of the engine being tested by altering the chemical reactions taking place in the engine. Vitiates can change the rates of chemical reactions or, in the extreme, the ability of the reaction to persist in the engine combustor. In order to translate the performance of an engine in a ground based facility to the expected performance in flight, the effects of facility vitiates must be determined.

This paper will discuss the progress of work which began in mid-2004 sponsored by the Office of the Secretary of Defense (OSD) Test & Evaluation/Science & Technology (T&E/S&T) Program. Contributors include the NASA Langley Research Center, George Washington University, North Carolina State University, the University of Pittsburgh, and the University of Virginia. The purpose of the work is to improve the state of the art of CFD capabilities for predicting the effects of the test media on the flameholding characteristics in scramjet engine combustors. The program has several components including the development of advanced algorithms and models for simulating engine flowpaths as well as a fundamental experimental and diagnostic development effort to support the formulation and validation of the mathematical models. The paper will provide details of current work involving the development of phenomenological models for Reynolds averaged Navier-Stokes codes, large-eddy simulation techniques, reduced-kinetics models, and two experiments with the associated nonintrusive diagnostics that will provide data for the modeling efforts.

Axisymmetric Coaxial Free Jet Experiment

Computational fluid dynamics (CFD) methods that employ the Reynolds-averaged Navier-Stokes (RANS) equations are widely used in the design and analysis of hypersonic airbreathing engine flow paths. These methods require models of statistical quantities of the turbulence in their development which have to be empirically calibrated and validated. In particular, new models for turbulent Schmidt and Prandtl number, as well as for turbulence-chemistry interactions, are required.[1] While suitable data is available for low-speed flows with combustion, it is still lacking in supersonic combustion. Goyne et al. report measurements using particle-imaging velocimetry of mean streamwise velocity in a dual-mode scramjet.[2] At the NASA Langley Research Center, several data sets have been acquired in a H_2 fueled supersonic combustor using the coherent anti-Stokes Raman spectroscopy (CARS)

technique[3] and the dual-Pump CARS technique.[4,5] The former technique gave temperature only while the latter gave both temperature and composition. Data included both mean flow and turbulent statistics, although the uncertainty in the latter was limited by both instrument precision and number of measurements from which the statistics were formed. International work in this area includes measurements in scramjet combustors conducted at ONERA (France) and DLR (Germany) using CARS,[6] and other non-intrusive techniques.

Available data are limited to only a subset of the important variables (which are temperature, composition, and velocity) in a limited number of geometries, and turbulence data are even rarer and of poor precision. To meet this need, we are developing an Interferometric Rayleigh Scattering technique for measuring instantaneous velocity to complement our Dual-Pump CARS technique.[7,8] This technique uses Rayleigh scattering from one of the CARS laser beams to measure velocity in the same instant that CARS measures temperature and composition. Details on the techniques are given in a later section. Analysis of streams of such instantaneous measurements allows us to form the statistical quantities (means, variances, covariances) required by the modelers.

Experimental facilities to provide suitable flow fields are being developed. An axisymetric coaxial free jet has been selected since it provides the good optical access required for the Rayleigh technique, and symmetry can be taken advantage of to minimize the number of spatial points required. (In order to form accurate statistics we need large numbers of measurements at each given point - the use of symmetry allows the total number of measurements to be made manageable.) Another requirement of the flow field is that it should provide data that is relevant to both H_2- and

hydrocarbon-fueled hypersonic air-breathing engines and the testing of such engines in ground facilities that employ vitiated air (the products of combustion of either H_2 or a hydrocarbon, enriched with O_2 to the same content as in air). The facility should be capable of providing flows of various Mach numbers, including supersonic, to establish the effects of compressibility. Finally, it is desirable to be able to create both supersonic combusting flows in which the flame is attached to the burner (flame held) and flows in which the flame is detached, since both types of flow are observed in hypersonic engine combustors.

Two sets of experiments are being performed. The second have essentially the same flow fields as the first, but are 6.35 times larger in scale. The first are conducted in the combustion laboratory in which the CARS and Rayleigh scattering techniques are being developed. The second will be conducted in NASA Langley's Direct Connect Supersonic Combustion Test Facility, and will provide data in which the turbulent eddy structures are better resolved spatially. In this paper we will discuss the experiments being conducted in the combustion laboratory.

Figure 1(a) shows the burner and nozzle, sectioned along the axis, without bolts, tubes, spark plug and other fittings shown; Figure 1(b) is an image of the facility near the nozzle exit during operation, showing the supersonic jet of vitiated air and the laser beams of the CARS-Rayleigh system. The facility consists of a water-cooled combustion chamber (burner), a silicon carbide nozzle (sonic convergent, or supersonic convergent-divergent for M=1.6 and M=2), with an exit diameter of 10 mm and a coflow nozzle. Various combinations of gas flows to the burner are possible. In one set of experiments, H_2 or CH_4 fuel, air and O_2 are reacted to provide vitiated air at various temperatures (dependent on flow rates). In these experiments,
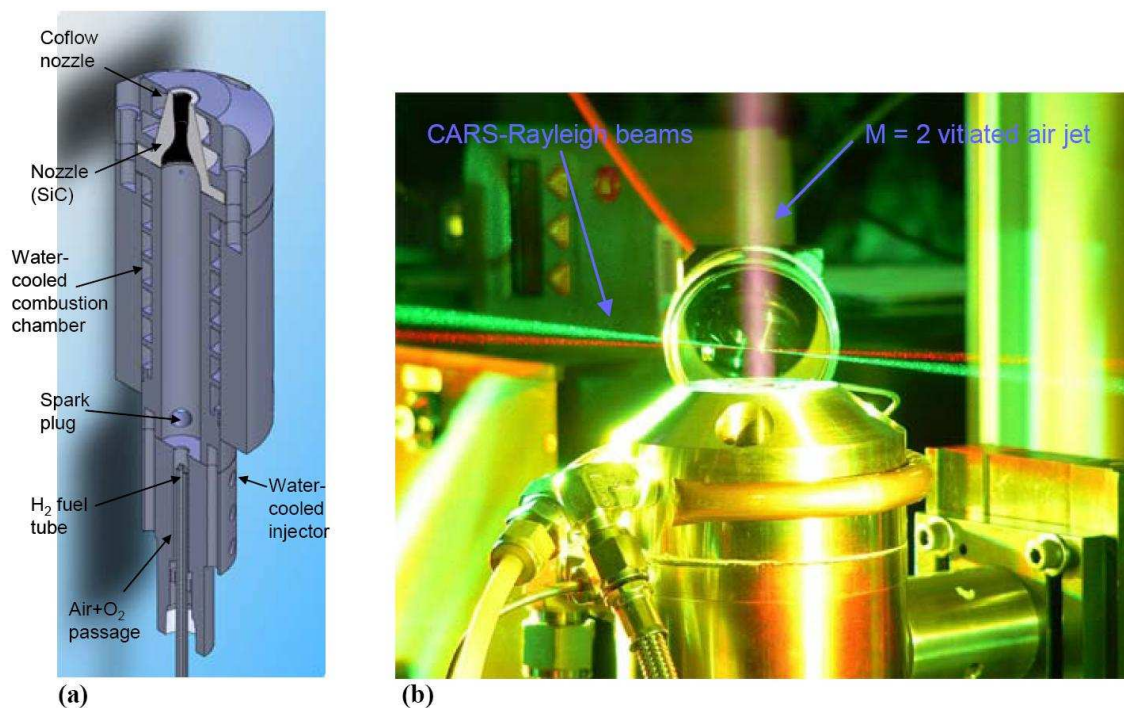
Figure 1: The supersonic jet combustor and nozzle. (a) Sectional view (without bolts, tubes, etc.). (b) Image during CARS-Rayleigh optical system data acquisition.

the coflow is of unheated H_2 or CH_4, and the result (depending on temperature) is a mixing and reacting coaxial jet flow. In another set of experiments, the gas flows to the burner are H_2, O_2 or N_2, and air in such a ratio that the products contain excess H_2. The coflow is of air and the result again is a mixing and reacting coaxial jet flow. Depending on temperature and on the co-flow rate, the flame may be held at the annular base region formed between the central and coflow nozzle exits where the flow recirculates.

Computational fluid dynamics (CFD) was used to help design both experiments. The first step of this effort was for the CFD specialist and experimentalist to work together to define a set of guidelines to ensure that the experiment provided a complete set of data that was useful for CFD model validation.[9] (Often times experimental data sets are in-complete, and as a result are of limited value for CFD validation.) This effort required the experimentalist to identify which properties could be measured, where they could be measured, and provide estimates of measurement accuracy. Similarly the CFD specialist identified the properties that were needed, where they were needed, and estimates of required accuracy. The CFD requirements were based on the CFD models to be validated in this effort (the turbulent mixing of chemical species and thermal energy). The experiment was then designed to capture the relevant physics of the models to be validated, to limit the complexity of the flowfield in order to exclude physical processes not relevant to the models being validated and to limit the sensitivity of the flowfield to properties which could not be readily measured.

As part of the design effort, a paramet-
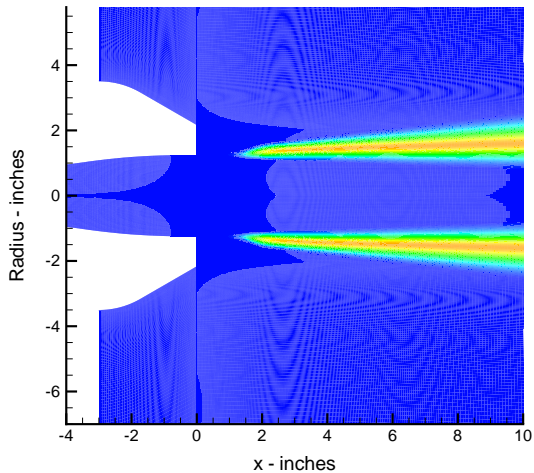
(a) No Co-flow Injection
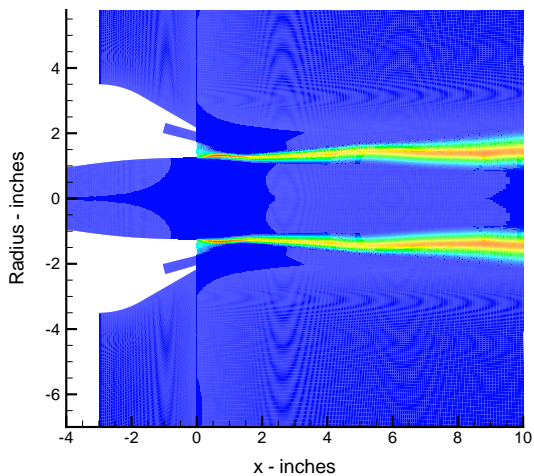
(b) 15° Co-flow injection

Figure 2: OH contours showing the sensitivity of the flame location to the presence of angled co-flow injection.

ric study of the proposed geometry and run conditions was conducted using CFD to determine the sensitivity of important experimental quantities to a number of variables including: inner jet temperature, flame holding base size, co-axial jet injection angle, inner jet Mach number and sensitivity to computational values of the turbulent Prandtl and Schmidt numbers. An example calculation using the Vulcan CFD code[10] is shown in Figure 2, which shows the sensitivity of the flame location to the presence of a co-flow. This flow is with a Mach 2, hot hydrogen-rich inner jet without and with cold air co-flow.

Once the experimental geometry was finalized, CFD was used to help define the experimental test matrix. This matrix, given in Table 1, includes variations in the inner jet Mach number, the temperature of the inner jet, the type of fuel (hydrogen or methane), the equivalence ratio of the fuel and air and the location of the fuel and air streams (inner jet or co-flow jet). The CFD calculations completed in this step will provide a baseline, using the standard constant Prandtl and Schmidt number models, to compare with the variable Prandtl and Schmidt number models described later in this paper.

Figure 3 contains tables and flow images showing the various types of flames that are observed in the actual experiment. Two types of images are shown: visible light (true color images) with a long exposure time, and false color infrared (IR) images acquired in the 8 - 9 micron (long wave) region at an exposure time of 10 ms. The tables contain information pertaining to the state of the flame: no flame, detached flame, flame held at the base or at the external coflow boundary, and if the flame holding is marginal, i.e., at the point of extinction. Figure 3(a) pertains to cases with H_2-vitiated air in the center jet and H_2 in the coflow. The center jet sensible enthalpy is varied by adjusting the flow rates from that

	Inner Jet			Outer Jet	
Mach No.	Heater Operation			Mach No.	Gas
1, 2	H_2+O_2+Air vitiated	no unreacted H_2	one $T_\circ$	off	-
1, 2	H_2+O_2+Air vitiated	H_2 rich	various $T_\circ$	off	-
1, 2	H_2+O_2+Air vitiated	H_2 rich	various $T_\circ$	≤ 1	Air
1, 2	H_2+O_2+Air vitiated	O_2 rich	various $T_\circ$	≤ 1	CH_4
1, 2	CH_4+O_2+Air vitiated	O_2 rich	various $T_\circ$	≤ 1	CH_4
1, 2	H_2+O_2+Air vitiated	O_2 rich	various $T_\circ$	≤ 1	H_2
1, 2	CH_4+O_2+Air vitiated	O_2 rich	various $T_\circ$	≤ 1	H_2

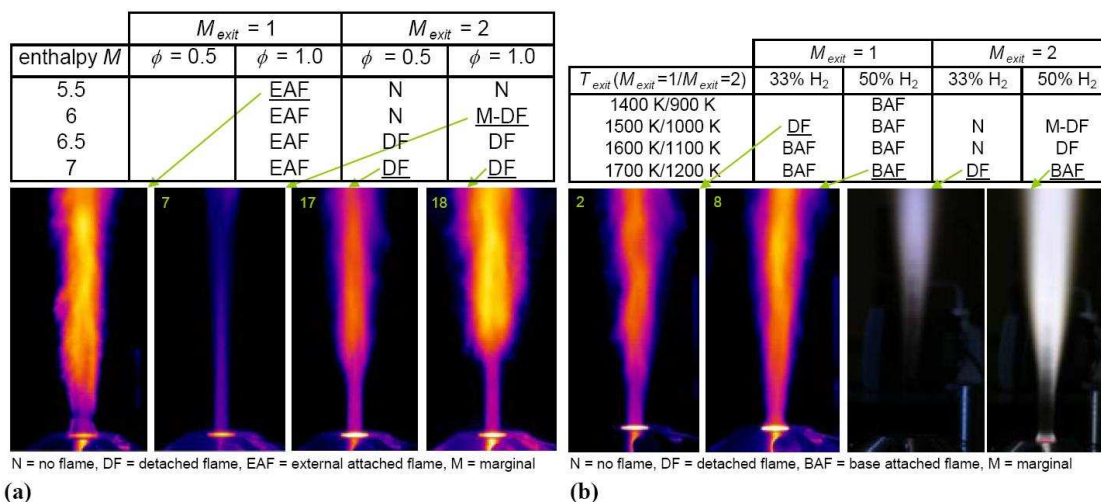Table 1: The experimental test matrix

Figure 3: Flame state for a matrix of supersonic operating conditions at sonic and Mach 2 pressure matched exit conditions. Mixed infrared (false color) and visible light images (two right-most images). (a) Vitiated air center jet with subsonic hydrogen air coflow at an overall equivalence ratio ϕ. (b) Hydrogen rich center jet with sonic coflow of air.

of Mach 5.5 flight to that of Mach 7, and the exit Mach number of the center jet is either 1.0 or 2.0. The coflow is subsonic at the nozzle exit and the equivalence ratio (the ratio of H_2 coflow rate to that required to consume all the O_2 in the center jet, ϕ) is either 0.5 or 1. (It is not implied that the coflow H_2 reacts only with the O_2 in the center jet.) For M_{exit} = 1, the flame is held at the exterior boundary in all cases, whereas, for M_{exit} = 2, in some cases there is no flame and in others the flame is detached (stands off from the nozzle exit), but there are no cases with flame holding. With a detached flame, the trend with increasing center jet enthalpy is for the flame to move towards the nozzle exit. Figure 3(b) pertains to cases with excess H_2 in the center jet, either 33% or 50% by volume of the jet flow being H_2. The exit static temperature is increased in increments of 100 K, and the exit Mach number is either 1.0 or 2.0. The coflow of air is sonic and pressure matched at the exit. In some cases, no flame is observed; in others, detached flames or flames attached at the base. The trend with increasing T_{exit} and decreasing M_{exit} is from no flame to detached flame to base-attached flame.

Simultaneous CARS and Interferometric Rayleigh Scattering

We have recently reported[11] and summarize here, the combination of a dual-pump coherent anti-Stokes Raman scattering system with an interferometric Rayleigh scattering system (CARS-IRS) to provide time-resolved simultaneous measurement of multiple properties in combustion flows. Time-resolved simultaneous measurement of temperature, absolute mole fractions of N_2, O_2, and H_2, and two components of velocity in a Hencken burner flame were performed to demonstrate the technique.

The experimental arrangement of the combined system is shown in Fig. 4. For the measurement of temperature and the absolute mole fractions of N_2, O_2, and H_2 we use a dual-pump CARS method.[4] The system uses spectrally-narrow green (injection seeded Nd:YAG at 532 nm) and yellow (NB Dye laser at 552.9 nm) laser pump beams and one spectrally broad red laser (BB Dye laser at 607 nm) beam as the Stokes beam.

The beams are combined at the focusing point of a spherical lens Lc (focal length of 410 mm) in a folded BOXCARS geometry to probe Raman transitions of N_2, O_2 and H_2. The input beams plus the coherent blue signal beam at 491 nm are collected and collimated by another spherical lens with the same focal length as Lc. The three input beams are captured in a beam dump while the blue signal beam is passed to a spectrometer. The CARS signal, which is a spectrally broad blue beam that contains N_2, O_2 and H_2 spectra, is analyzed by a spectrometer and recorded by the CCD1 camera. The shape of these spectra provides information on the temperature while the relative intensities of these spectra provide a measure of the relative mole fractions. The spectrum is fit with a theoretical model to determine the temperature and mole fractions.

The velocity measurement is performed simultaneously using an interferometric Rayleigh scattering measurement system.[7] The same pulsed, seeded green laser beam employed in the CARS technique is used as a narrow-band light source for the Rayleigh scattering system. The receiving optics for Rayleigh scattering are designed to capture the Rayleigh scattered light from the green pump beam in the measurement volume while preserving the scattering angle information, and to mix it together with the unshifted light of the laser before it is passed through the interferometer. In this
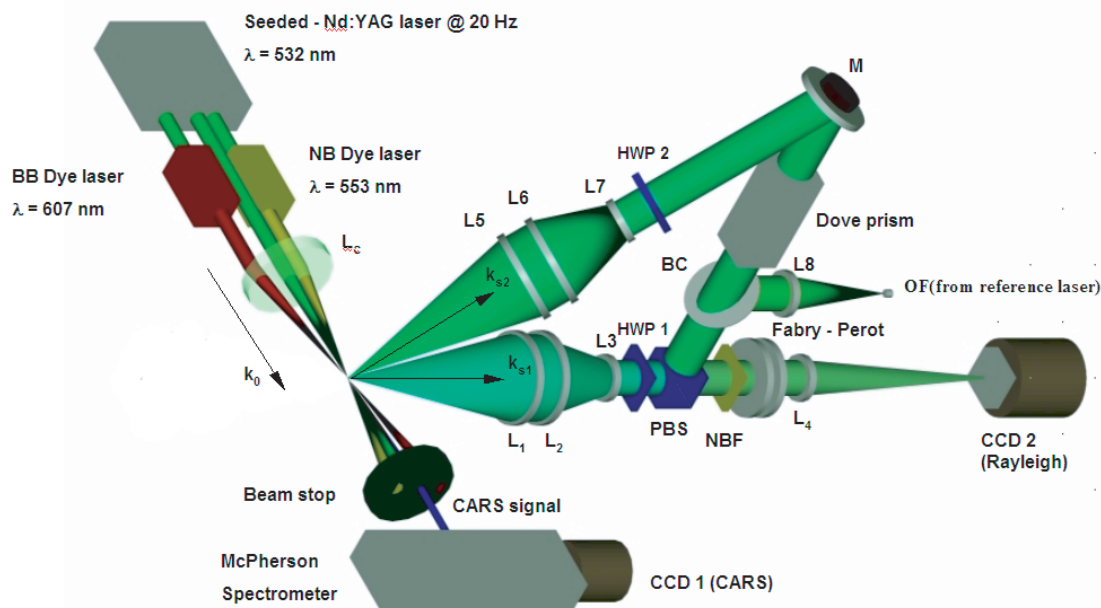
Figure 4: Experimental setup of the combined CARS - IRS system

way more than one component of velocity at multiple points can be measured in one interferogram.[7,12] The velocity components measured are those that bisect the angles of laser's incidence and the collection optics. Since two directions are collected, two velocity components are measured. The Rayleigh scattered light from the two measurement directions are combined with a polarizing beam splitter (PBS) and directed through a Fabry-Perot etalon and onto a CCD camera for analysis (CCD2). The particular setup used here gives a range of measurable velocities from 0 to ~3 km/sec up to temperatures of about 2500 K. The CARS spectra and the Rayleigh spectra are acquired simultaneously by synchronizing the cameras with the green laser Q-switch pulse at 20 Hz. The spectra are subsequently processed, as described in reference 11 to determine the temperature, composition and velocity.

To demonstrate the method, experiments were carried out in a Hencken burner, which provides an adiabatic H_2-air atmospheric pressure flame. The flame was stabilized with a co-flow of N_2. This flame was used because it provided a challenging high-temperature measurement environment while producing a known (near-zero) velocity.

Simultaneous CARS and Rayleigh scattering spectra up to 1610 K are shown in Fig. 5 (a-c) and in Fig. 5 (d-f), respectively: (a) and (d) are in the co-flow of N_2, (b) and (e) are in a high temperature flow containing N_2 and O_2, and (c) and (f) are in a high temperature flow containing N_2 and a low proportion of O_2. The CARS spectral plots show the experimental data, the theoretical fits, and also the residual between them. These spectra were used to calculate the vibrational gas temperature and the mole fraction of H_2, O_2,
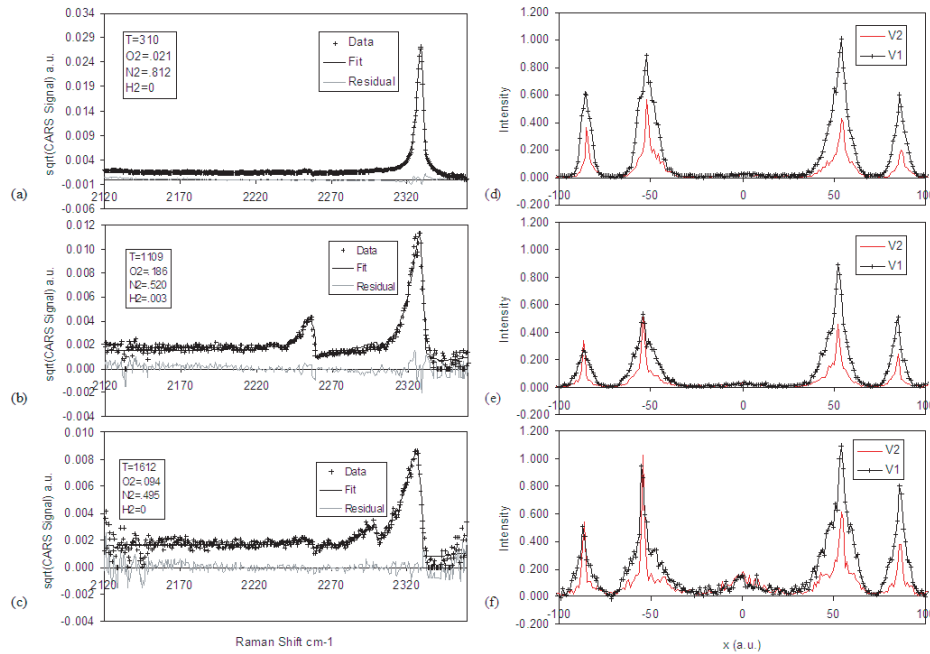
Figure 5: Simultaneous spectra of CARS (left) and Rayleigh scattering from two viewing directions (right). The CARS spectra are both data and fits of theory to the data. The Rayleigh spectra are data points connected by lines

and N_2.

For the Fabry-Perot spectra shown in Fig. 5, only one fringe order from each spectrum has been analyzed for this paper. The narrow shaped peak, more visible in the spectra of higher temperature, is the reference laser frequency (no Doppler shift). The broader spectrum is the Rayleigh scattered light. Each figure contains two Rayleigh and two reference spectra corresponding to the two collecting directions V1 (black trace) and V2 (red trace of smaller amplitude), differing by 34 degrees. Two-component velocity measurements in the range of 300-1600 K showed near-zero velocities (< 30 m/s) and standard deviations of 30-40 m/s. These errors are about 1% of the dynamic range of this measurement system (3,000 m/s). Measurement of one velocity component was shown to be possible at up to $\sim$2,400 K with this system. These accuracies and precisions are within

the desired range required for the planned supersonic combustion experiments where velocities will be up to 1,500 m/s. However, it is anticipated that future improvements in both hardware and software will allow these errors to be reduced by a factor of two or more.

A Response Surface Methodology Approach to Refine Computational Models Using Experimental Data

Improved numerical simulation of hypersonic engine performance relies on the development of enhanced codes with an increased capability to model turbulence, turbulent mixing, and kinetics. The validation phase of these numerical models requires the comparison of simulated results to experimental data obtained from multiple experimental cases. One aspect of validation, re-

ferred to as model refinement, involves the selection of model tuning parameters to achieve the *best* agreement with the experimental data.[13]

In this section, we propose a response surface methodology (RSM) approach to select the values of the model tuning parameters. For over 50 years,[14] RSM has been used to successfully characterize and optimize industrial and scientific products and processes. In general, RSM is a strategy to efficiently identify important factors in an experimental system and to specify the settings of those factors that improves a measure of system performance. It is applicable to both physical experimental systems and computational simulation.

The model refinement phase is essentially an experiment in which we set specific values of the model tuning parameters, execute the simulation, measure the correlation to experimental results, and seek to find the values of the parameters that improve the correlation, or agreement, with actual experimental measurements. In the RSM context, the model tuning parameters are the *factors* with associated *levels*, which represent their numerical values. The simulation-to-experimental correlation forms the *response* that we seek to improve. Applying RSM offers a general, systematic approach to perform model refinement that emphasizes the use of minimal computational resources and features an analysis approach to gain deeper insights into the underlying physics. For more information on statistical experimental design and RSM, see Refs. 15, 16.

The first step in the RSM approach is to choose the model tuning parameters (factors) to be varied and their high and low levels, or range. Then, an *experimental design* is constructed that specifies the levels and combinations of factors to be run through the sim-

Model Tuning Parameters					
Run	C_Y	C_{Y2}	C_{Y3}	C_{Y41}	C_{Y7}
1	-1	-1	-1	-1	1
2	1	-1	-1	-1	-1
3	-1	1	-1	-1	-1
4	1	1	-1	-1	1
5	-1	-1	1	-1	-1
6	1	-1	1	-1	1
7	-1	1	1	-1	1
8	1	1	1	-1	-1
9	-1	-1	-1	1	-1
10	1	-1	-1	1	1
11	-1	1	-1	1	1
12	1	1	-1	1	-1
13	-1	-1	1	1	1
14	1	-1	1	1	-1
15	-1	1	1	1	-1
16	1	1	1	1	1
17	0	0	0	0	0

Table 2: Initial Experimental Design (+/-1 represent high and low levels of each factor in coded units, 0 represents the mid-point)

ulation model. For each combination of factors, known as an *experimental run*, measures of simulation-to-experimental agreement (responses) are obtained. From these data, parametric *validation models* of the relationship between the factors and the responses are estimated. These validation models describe a multidimensional *validation surface* of the difference between the simulated and experimental results as a function of the model tuning parameters. Our goal is to identify the regions of the validation surface (combination of factors) that represent agreement with the experimental results. Since the functional form of the validation surface is unknown, an iterative process is performed to assess the adequacy of an estimated validation model and augment the experimental design as required, thereby enabling the estimation of a higher fidelity model. Once adequate models are found, they are com-

bined to perform multiple response optimization, thereby enabling the determination of the values of the model tuning parameters to achieve the *best* correlation to the experimental data for all of the response quantities of interest. Note that we use the term *best* to describe a trade-off among multiple competing criteria in correlating different aspects of the simulation model.

In the final step, the values of the model tuning parameters determined by the optimization are run through the simulation code to confirm that the predicted quality of correlation with the experimental results is obtained. This confirmation phase provides confidence in the estimated validation models and the optimization results.

As an example of the initial setup of this proposed approach, consider the development of a variable turbulent Schmidt number formulation,[17] described in the next section, to model a Helium co-flow mixing experiment.[18] Five model tuning parameters (C_Y, C_{Y2}, C_{Y3}, C_{Y41}, C_{Y7}) that proportionally scale specific terms within the turbulence equation, are varied at three levels; a high, middle, and low setting. The initial experimental design requires $2^{5-1} = 16$ factorial combinations of the five factors at their high and low levels, representing a one-half fraction of all possible combinations. In addition, the design includes one combination with all 5 factors simultaneously set at their middle level. The design is provided in Table 2 in coded units. Geometrically, the design is a subset of vertices of a five-dimensional hypercube and a design point in the center of the hypercube.

This design supports the efficient and unique estimation of a first-order model given by

$$y = \beta_0 + \sum_{i=1}^{k} \beta_i x_i + \sum_{i=1}^{k-1} \sum_{j=i+1}^{k} \beta_{ij} x_i x_j + \varepsilon,$$

where y is the response (validation metric), x

is the level of the factors (model tuning parameters), β's are the validation model coefficients, ε is the residual error in fitting the model, k is the number of parameters (factors) in the experiment. Typically in these types of simulation codes, ε is a systematic error rather than a random error due to the deterministic nature of the simulation.

An important feature of this model is that it allows for the modeling of interactions between the factors, represented by the β_{ij} terms. If the effect on the response by changing the value of one of the model tuning parameters depends on the setting of another parameter value, then we say that the factors interact. Synergistic and antagonistic interaction effects are common in many applications and cannot be captured if the factors are varied one at a time rather than simultaneously in a factorial arrangement. Identifying interactions often provides new insights into the underlying physics of the experimental system.

In this example, the four system response quantities[19] (SRQ) considered are species mass fraction, velocity, Pitot pressure, and total temperature measured throughout the flow field. Typically, the correlation to experimental results involves a subjective, qualitative review of plots. However, a quantitative measure of correlation quality is required that has the form of $\mathbf{VM} = f(\mathbf{y}_c - \mathbf{y}_e)$, where $\mathbf{VM}$ is the validation metric vector, $\mathbf{y}_c$ is the SRQ from the computational model, and $\mathbf{y}_e$ is the SRQ from the experimental data. Note that $\mathbf{y}$ is a vector containing the values of the responses at the location in the flow field where experimental measurements were obtained. At this stage in the development of the approach, a simple L_2 norm of $\mathbf{VM}$ is proposed to provide a numerical measure of the agreement with the experimental results. A full development of this case study will be presented in a subsequent paper.

In summary, the proposed RSM approach to model refinement is expected to offer a general, structured approach to obtain values for the model tuning parameters. In addition, due to the structured nature of the approach, the selection of the tuning parameters will be reproducible by other researchers. A particular strength of the approach is its straightforward extension to higher-dimensional factor spaces and its ability to incorporate multiple experimental cases, thereby providing a set of parameters that are adequate over a range of experimental conditions.

Figure 6: Schematic of Experiment Setup

Improved Turbulence Models for Reacting Flows

The research to improve the modeling of turbulent transport of heat and mass has resulted in a tentative turbulence model where the turbulent Prandtl (Pr_t) and Schmidt (Sc_t) numbers are calculated as part of the solution and where reactions involving chemical source terms are modeled. The turbulent Prandtl and Schmidt numbers are obtained by solving additional equations for the variance of enthalpy and its dissipation rate; and for the variance of concentrations and their dissipation rate. The resulting equations, together with modeling of terms involving chemical source terms, are given in the references .[17] It is to be noted that the model avoids the use of assumed or evolution PDF's to account for chemistry/turbulence interactions.

Two sets of H_2/Air chemical kinetic mechanisms are considered: the seven species/seven reaction model of Jachimowski ,[21] where the reaction rates are functions of temperature; and the nine species/nineteen reaction model of Connaire, et al.[22] where the reaction rates are functions of both pressure and temperature.
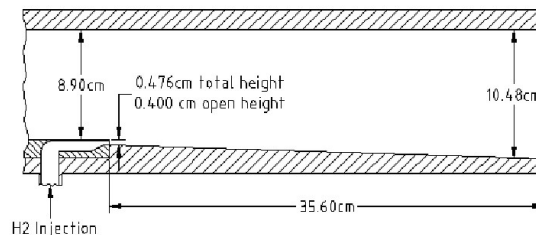
The predictions from the model are com-

pared with two sets of experiments involving supersonic mixing [23,24] and combustion.[24] Only results involving combustion will be presented here. Results involving mixing are given in Ref. 17. A schematic of the experiment of Burrows and Kurkov [24] is shown in Fig. 6. Hydrogen is injected into the test section at Mach M=1 through a nickel injector parallel to the vitiated main flow. At the entrance of the test section, M = 2.44, the state pressure is one atmosphere, and the static temperature is in the range 1250-1270K. Hydrogen is injected at a total temperature slightly above the ambient temperature. All comparisons are made at the test section exit plane, which is 35.6 cm from the hydrogen injection step. Three sets of figures are presented. For the first two sets, Jachimowski's model is employed. In the first set, terms involving averages of chemical source terms, which represent the turbulence-chemistry interactions, are ignored, while in the second, the contributions of these terms are included. As is seen from Fig. 7, poor agreement with experiment is indicated. Figures 8 and 9 show contours of Sc_t and Pr_t. It appears that the main source of the discrepancy is a result of reduced Pr_t near the mixing region. This has the tendency of promoting heat transfer and early combustion. Figure 10 shows that when turbulence-chemistry interactions are included, much better agreement with ex-
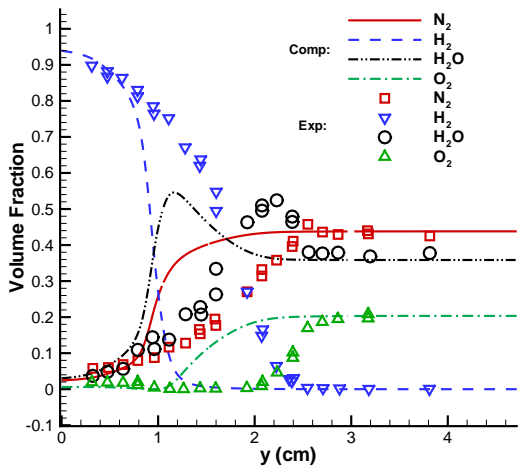
Figure 7: Comparison of Computed and Measured Volume Fraction, with Chemical Source Term, Jachimowski's 7 Species/7 Reactions Model
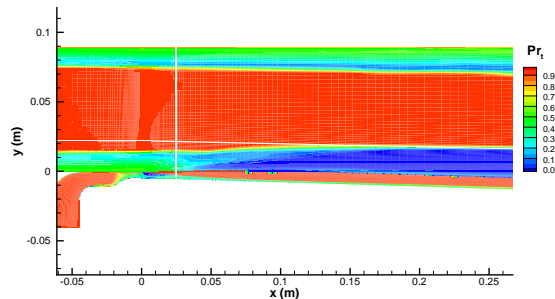

Figure 9: Prandtl Number Contours, without Chemical Source Term, Jachimowski's 7 Species/7 Reactions Model
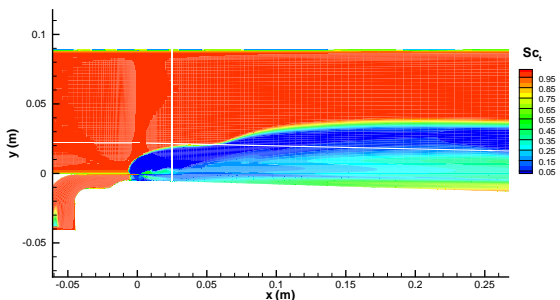

Figure 8: Schmidt Number Contours, without Chemical Source Term, Jachimowski's 7 Species/7 Reactions Model
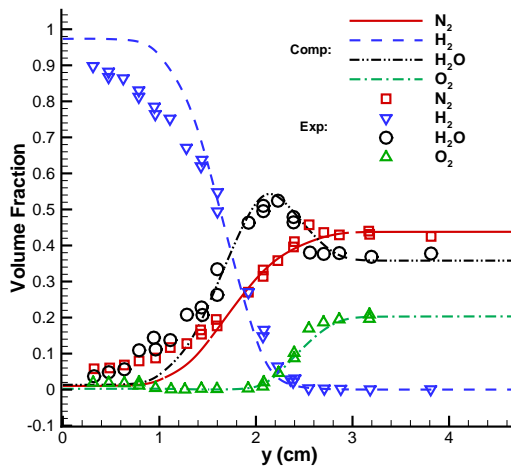

Figure 10: Comparison of Computed and Measured Volume Fraction, with Chemical Source Term, Jachimowski's 7 Species/7 Reactions Model
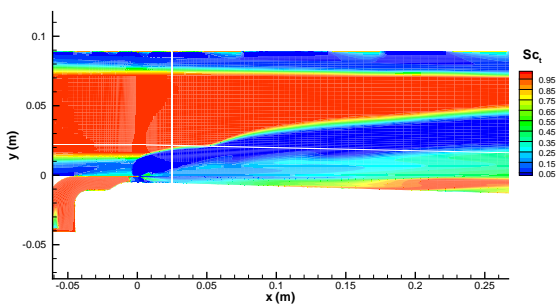
Figure 11: Schmidt Number Contours, with Chemical Source Term, Jachimowski's 7 Species/7 Reactions Model
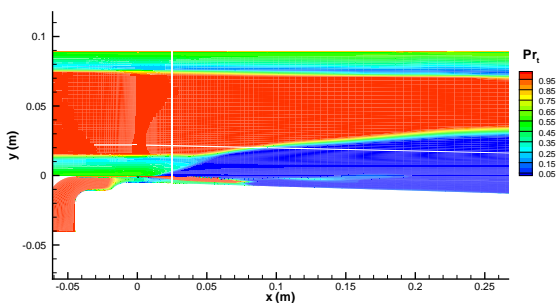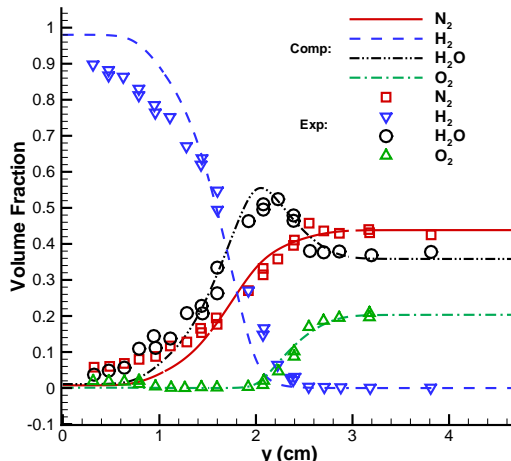

Figure 13: Comparison of Computed and Measured Volume Fraction, with Chemical Source Term, Connaire *et al* 9 Species/19 Reactions Model

Figure 12: Prandtl Number Contours, with Chemical Source Term, Jachimowski's 7 Species/7 Reactions Model

periment is indicated. Figures 11 and 12 show contours of Sc_t and Pr_t. In the third set, Figures 13-15 show the prediction of Connaire[22] et al. model. As is seen from Fig. 13, good agreement with experiment is indicated. This suggest that modeling approaches can serve as a substitute for approaches employing evolution PDF's. The differences in the Sc_t contours of Figs. 11 and 14 illustrate the fact that, in regions where mixing does not play a role, the value of diffusion coefficient has little influence on the final results.

Based on the above results, two relevant observations can be made. The first is that modeling of averages of terms involving chemical source terms is a viable option. When this approach is compared with approaches requiring assumed or evolution PDF's, a great deal of computational efficiency is achieved. Second, a relatively inexpensive calculation of variable Pr_t and Sc_t can be obtained by assuming a value for the Lewis number, and eliminating either the
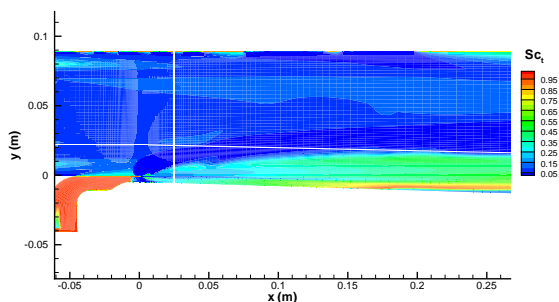
Figure 14: Schmidt Number Contours, with Chemical Source Term, Connaire *et al* 9 Species/19 Reactions Model
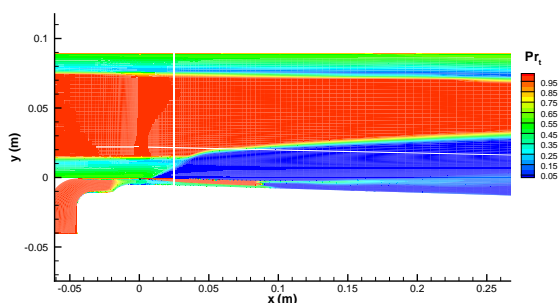

Figure 15: Prandtl Number Contours, with Chemical Source Term, Connaire *et al* 9 Species/19 Reactions Model

equation for the enthalpy variance and its dissipation rate, or those for the variance of concentrations and its dissipation rate. This, however, will result in ignoring one of the averages involving chemical source terms. Because inclusion of such terms is important, assuming a constant Lewis number is not recommended.

Large Eddy Simulation of Reacting Flows

It is now widely recognized that one of the most convenient means of predicting the unsteady physics of turbulent reacting flows is via large eddy simulation (LES).[34] A serious issue in such simulations is accurate modeling of the subgrid scale (SGS) quantities. While this issue is important in any LES, it is particularly difficult when dealing with reacting flows .[28] The filtered density function (FDF) has proven particularly effective for accurate SGS modeling in reacting flows.[32] This method is the counterpart of the probability density function (PDF) methodology, which has been long-established in RANS calculations of turbulent combustion .[38] A reliable means of determining the FDF is via solution of its transport equation. A systematic study in this endeavor was initiated by Colucci *et al.*[29] who developed and solved a modelled transport equation for the marginal scalar FDF (SFDF) in constant density reacting flows. The extension of this work was conducted by Jaberi *et al.* [33] who developed the marginal scalar filtered mass density function (SFMDF). This is essentially the mass-weighted form of the SFDF. Due to the marginal nature of the FDFs in these studies, all of the hydrodynamic effects including all of the velocity-scalar correlations are modelled via conventional (non-FDF) methods. The extension for modeling of the velocity field was done by Gicquel *et al.*[31] who developed and solved a transport equation for the mar-

ginal velocity FDF (VFDF) in constant density flows. This work demonstrated some of the advantages of the FDF in comparison to conventional methods in accounting for the effects of SGS velocity correlations. The most general formulation, is the joint FDF of the velocity and the scalar fields (VSFDF) in constant density flows.[41]

The objective of this part of the work is to extend the capabilities of the FDF methodology for LES of the flows considered in the other parts of this investigation. To achieve this objective, our work has been concentrated on two main tasks: (1) Development of the joint velocity-scalar filtered mass density function (VSFMDF), and (2) Application of the SFMDF for prediction of complex turbulent combustion systems. The work in (1) was motivated simply because of the physics of high speed turbulent combustion which require variable density formulation. The work in (2) was motivated in our continuing attempt to extend the boundaries of applicability of the FDF method.

In the work pertaining to (1), an exact transport equation is derived for the VSFMDF. It is shown that the effects of SGS convection and chemical reaction appear in closed form in this equation. The unclosed terms in this equation are modelled in a fashion similar to that typically used in RANS. A set of stochastic differential equations (SDEs) are considered which yield statistically equivalent results to the modelled VSFMDF transport equation. The SDEs are solved numerically by a Lagrangian Monte Carlo procedure in which the Itô-Gikhman character of the SDEs is preserved. The consistency of the proposed SDEs and the convergence of the Monte Carlo solution are assessed. In nonreacting flows, it is shown that the VSFMDF results agree well with those obtained by a "conventional" finite-difference LES procedure in which the transport equations corresponding to the filtered quantities are solved directly. The VSFMDF results are also compared with those obtained by the Smagorinsky closure, and all the results are assessed via comparison with data obtained by direct numerical simulation (DNS) of a temporally developing mixing layer involving transport of a passive scalar. It is shown that all the first two moments including the scalar fluxes are predicted well by the VSFMDF. In these simulations, the VSFMDF methodology is shown to be able to represent the variable density effects very well. The VSFMDF predictions of shear layer growth rate for various density ratios compare well with DNS data. The predictive capabilities of the VSFMDF in reacting flows are further demonstrated by LES of reacting shear flows. The predictions show favorable agreements with laboratory data,[36] and demonstrate several of the features as observed experimentally. For details of this work, we refer to a recent Ph.D. Dissertation by Sheikhi[39]

In the work pertaining to (2) the SFMDF is applied for LES of a turbulent bluff-body stabilized hydrogen-methane jet flame. This flame is studied by the Combustion Research Facility at the Sandia National Laboratories and the Thermal Research Group at the University of Sydney.[25,26,35] This work was promoted in the wake of our recent success[40] in SFMDF predictions of the simpler piloted jet flame experiments of Sandia.[25,27,37] For this flame (which exhibits little local extinction), a simple flamelet model is used to relate the instantaneous composition to the mixture fraction. The modelled SFMDF transport equation is solved by a hybrid finite-difference/Monte Carlo scheme. The results via this method capture important features of the flame as observed experimentally. In fact, all of the results including the means, RMS values and PDFs of the scalar field as predicted by SFMDF compare very well with

experimental data. For details of this work, we refer to a recent Ph.D. Dissertation by Drozda [30]

Reduced Chemical Kinetics Models

While turbulent transport and turbulent reaction models are system dependent (eg. inflow turbulent intensity), the fundamental *laminar reaction models* can be investigated independent of the actual reaction flow field by analyzing the models under relevant physical time scales. In particular, the present effort is focused on the development of reduced reaction models based on laminar kinetic effects on ignition/propagation/extinction of hydrocarbon-air mixtures and subsequent application to turbulence-chemistry models.

Because of the importance of ethylene in many hydrocarbon oxidation pathways, both elementary[42] as well as *ad hoc*[43] models have been developed to describe the ignition and oxidation processes. Based on the elementary models, systematically derived reduced reaction models have also been developed for engineering applications; however, these models have focused on describing either the propagation of premixed flames and extinction of nonpremixed flames [44] or ignition.[45] In general, reduced reaction models developed for flame propagation and extinction cannot be applied to the prediction of ignition phenomena because some of the key initiation elementary steps necessary for ignition phenomena may be missing or transport effects are not included in ignition analysis. As part of the present work, a general methodology has been developed to address above shortcomings, as described below.

In early investigations using reduced reaction models based on the quasi-steady-state (QSS) approximation, the computational efficiency was not a primary factor in developing these reduced models. For example, highly-stiff coupled algebraic relations arising from the QSS approximation were solved iteratively, i.e. with "inner" iterations, or the coupled QSS algebraic relations were truncated to yield "explicit" expressions for the species in QSS, albeit within a narrow range of validity or with diminished accuracy.[46] The formal computer based reduction methods, e.g. computational singular perturbation (CSP) method of Lam,[47] computer-aided reduction method (CARM) of Chen,[48] and intrinsic low-dimensional manifold (ILDM) method of Pope,[49] facilitated the development of reduced reaction models for large detailed models. However, these mathematical/computational approaches still require the solution of highly-stiff algebraic relations using computationally expensive "inner" iterations. The automatic mechanism reduction procedure developed here (based on the MATLAB programming language), can relax certain QSS relationships to obtain "explicit" expressions for the QSS species, i.e. avoid costly "inner" iterations. The level of relaxation can be based on a predetermined threshold satisfying the QSS approximation. Unlike other automated reduction procedures, the present explicit reduced reaction modeling (ERRM) approach can be applied to ignition phenomenon as well as premixed and non-premixed flames .[50] In this regard, the present MATLAB-based ERRM approach is more general compared to the CSP approach.[47]

Figures 16 and 17 show a typical comparison of the ignition delay for C_2H_4-air and H_2-air mixtures, while Fig. 18 shows a comparison of premixed flame propagation velocity predictions for CH_4-air mixtures based on two reduced reaction models developed for C_2H_4. Also shown are the results using Wang's[42] detailed kinetic model with 73 species and 469 reactions and a skeletal model

Figure 16: Comparison of ignition delay predictions of stoichiometric C2H4-air mixture as a function of temperature
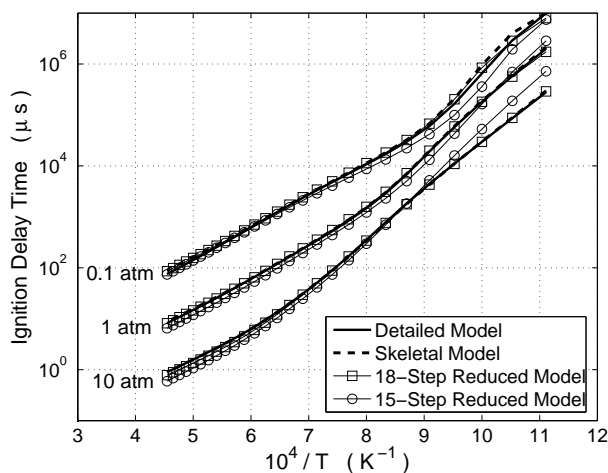

Figure 17: Comparison of ignition delay of predictions of stoichiometric H2-air mixture as a function of temperature

developed consisting of 31 species and 128 reactions. The 15-step reduced reaction model is based on flame propagation of C_2H_4-air flames, while the 18-step reduced reaction model is based on C_2H_4-air ignition delay .[50]

To demonstrate the robustness of reduced reaction models, the current 15-step and 18-step models are used in predicting the flame extinction condition of C_2H_4 and air non-premixed flame, with the air-stream heated to 900 K using a typical vitiation facility (eg. iso-butane preheater with vitiated air composition of $X_{O2} = 0.21$, $X_{N2} = 0.727$, $X_{CO2} = 0.028$, and $X_{H2O} = 0.035$). As shown in Fig. 19, the extinction strain rate is reduced because of the vitiation species CO_2 and H_2O included in the model and the 18-step reduced reaction model can capture the same trend as the skeletal model. In the future, effects of other intermediate species in vitiation facilities on ignition and flame propagation and extinction will be analysed.

Concluding Remarks

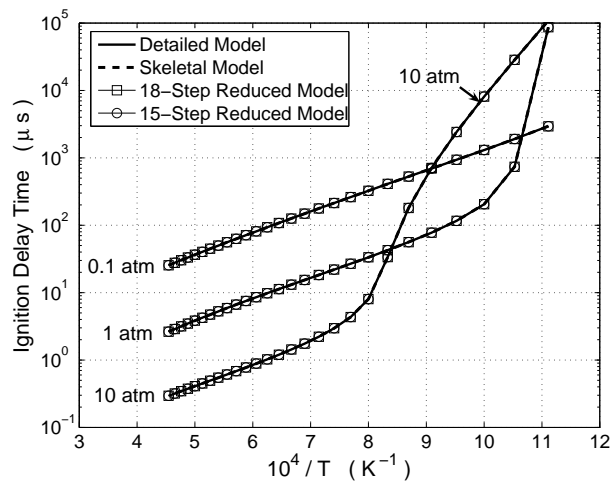This paper has described work involving the development of phenomenological models

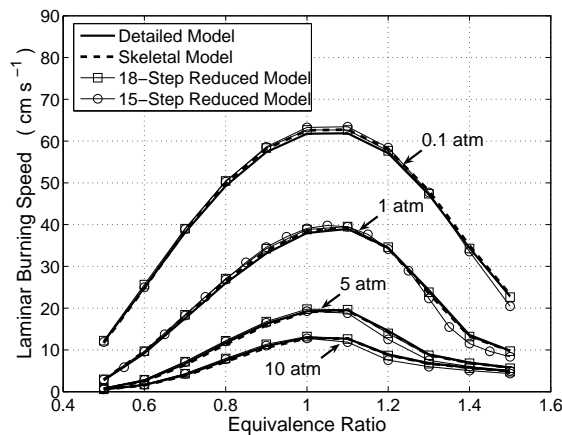
Figure 18: Comparison of laminar burning velocity of premixed CH4-air mixture as a function of equivalence ratio, at $T_0=300K$
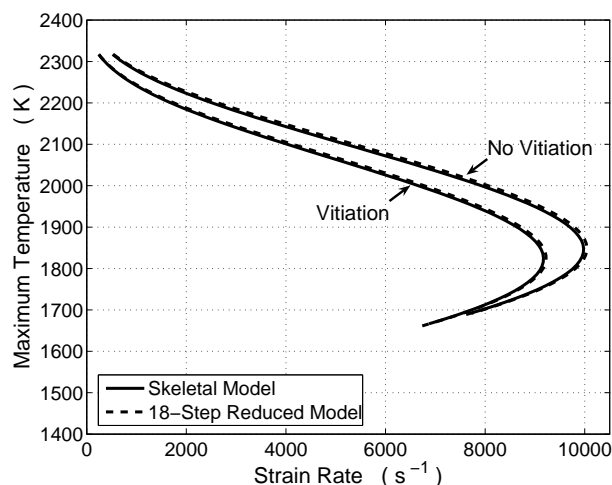
Figure 19: Comparison of peak flame temperature prediction of C2H4 and air non-premixed flame with flow strain rate, with air preheated to 900 K using a vitiated facility

for Reynolds averaged Navier-Stokes codes, subgrid scale models used in large-eddy simulation and reduced-kinetics models to study the effects of vitiation on engine testing in combustion heated facilities. Two fundamental experiments are being performed to provide data that will be used in the development and refinement of these models. Experimental data is extracted from the experiments using nonintrusive diagnostics that allow accurate simultaneous measurement of temperature, species, and up to three components of velocity in supersonic flow without changing the character of the flowfield. Once the databases are in hand, the data is analyzed using a response surface methodology that provides an efficient means of determining critical parameters in a chosen model. The models will then be incorporated into combustion codes used in engine flowpath analysis and design.

Acknowledgement

References

[1] Baurle, R.A., "Modeling of High Speed Reacting Flows: Established Practices and Future Challenges," AIAA 2004-267, 42nd Aerospace Sciences Meeting and Exhibit, Reno, NV, 5-8 Jan, 2004.

[2] Goyne, C.P., McDaniel, J.C., Krauss, R.H., Day, S.W., "Velocity measurement in a dual-mode supersonic combustor using particle image velocimetry," AIAA Paper 2001-1761, AIAA/NAL-NASDA-ISAS International Space Planes and Hypersonic Systems and Technologies Conference, 10th, Kyoto, Japan, Apr. 24-27, 2001.

[3] Cutler, A.D., Danehy, P.M., Springer, R.R., O'Byrne, S., Capriotti, D.P., De-Loach, R., "Coherent Anti-Stokes Raman Spectroscopic Thermometry in a Supersonic Combustor," AIAA J., Vol. 41, No. 12, Dec. 2003.

[4] O'Byrne, S., Danehy, P.M., Cutler, A.D., "Dual-Pump CARS Thermometry and Species Concentration Measurements in a Supersonic Combustor," AIAA Paper 2004-0710, 42nd Aerospace Sciences Meeting, Reno, NV, Jan. 5-8, 2004.

[5] Tedder, S. A., O'Byrne, S., Danehy, P. M., Cutler, A. D., "CARS Temperature and Species Concentration Measurements in a Supersonic Combustor

with Normal Injection," AIAA Paper 2005-0616, 43rd AIAA Aerospace Sciences Meeting, Reno, NV, Jan 10-13, 2005.

[6] Bresson, A., Bouchardy, P., Magre, P., Grisch, F., "OH/acetone PLIF and CARS thermometry in a supersonic reactive layer," AIAA Paper 2001-1759, AIAA/NAL-NASDA-ISAS International Space Planes and Hypersonic Systems and Technologies Conference, 10th, Kyoto, Japan, Apr. 24-27, 2001.

[7] Bivolaru, D., Danehy, P.M., Lee, J.W., Gaffney, R.L., Cutler, A.D., "Single-pulse, Multi-point Multi-component Interferometric Rayleigh Scattering Velocimeter," AIAA-2006-0836, 44th AIAA Aerospace Sciences Meeting, Reno, NV, 9-12 Jan., 2006.

[8] Bivolaru, D., Otugen, M. V., Tzes, A. and Papadopoulos, G., "Image Processing for Interferometric Mie and Rayleigh Scattering Velocity Measurements," AIAA Journal, Vol. 37, No. 6, pp. 688-694, 1999.

[9] Gaffney, Richard L. Jr., Cutler, Andrew D., "CFD Modeling Needs And What Makes A Good Supersonic Combustion Validation Experiment," JANNAF CS/APS/PSHS/MSS Joint Meeting, Charleston, SC, June, 2005.

[10] White, J. A. and Morrison, J. H., "A Pseudo-Temporal Multi-Grid Relaxation Scheme for Solving the Parabolized Navier-Stokes Equations," AIAA paper no. 99-3360, June, 1999.

[11] D. Bivolaru, P. M. Danehy, K. D. Grinstead, Jr., S. Tedder, A. D. Cutler, "Simultaneous CARS and Interferometric Rayleigh Scattering," AIAA AMT-GT Technology Conference, San Francisco, AIAA-2006-2968 June (2006).

[12] Bivolaru, D., Danehy, P. M., and Lee, J. W, "Intracavity Rayleigh-Mie Scattering for multipoint, two-component velocity measurement," Optics Letters, Vol. 31, No. 11, pp. 1645-1647, June, 2006.

[13] Cutler, A. D., Danehy, P. M., Byrne, P.O., Rodriguez, C.G., and Drummond, J. P., "Supersonic Combustion Experiments for CFD Model Development and Validation," AIAA 2004-0266, 2004.

[14] Box, G.E.P. and Wilson, K.B., "On the Experimental Attainment of Optimum Conditions," *Journal of the Royal Statistical Society* Ser.B, 13, pp. 195–241, 1951.

[15] Montgomery, D. C. , *Design and Analysis of Experiments, 6th edition*, John Wiley & Sons, 2004.

[16] Myers, R. H. and Montgomery, D. C., *Response Surface Methodology: Process and Product Optimization Using Designed Experiments, 2nd edition*, John Wiley & Sons, 2002.

[17] Xiao, X. , Edwards, J.R., Hassan, H.A., and Cutler, A.D., "Variable Turbulent Schmidt Number Formulation for Scramjet Applications," *AIAA Journal*, 44(3), pp. 593–599, 2006.

[18] Cutler, A. D., Diskin, G. S., Danehy, P. M., and Drummond, J. P., "Fundamental Mixing and Combustion Experiments for Propelled Hypersonic Flight," AIAA 2002-3879, 2002.

[19] Oberkampf, W.L. and Barone, M.F. , "Measures of Agreement Between Computation and Experiment: Validation Metrics,"AIAA 2004-2626, 2004.

[20] Xiao, X., Hassan, H. A., and Baurle, R. A., "Modeling Scramjet Flows with Variable Turbulent Prandtl and Schmidt Numbers," AIAA Paper 2006-0128.

[21] Jachimowski, C. J., "An Analytic Study of Hydrogen-Air Reaction Mechanism with Application to Scramjet Combustion," NASA Technical Papr 2791, February 1988.

[22] Connaire, M. O., Curran, H. J. Simmie, J. M., Pitz, W. J., and Westbrook, C. K., "A Comprehensive Modeling Study of Hydrogen Oxidation," International Journal of Chemical Kinetics, Vol. 36, 2004, pp. 603-622.

[23] Cutler, A. D., Carty, A. A., Doerner, S. E., Diskin, G. S., and Drummond, J. P., "Supersonic Coaxial Jet Flow Experiment for CFD Validation," AIAA Paper 1999-3388, July 1999.

[24] Burrows, M. C. and Kurkov, A. P., "Analytical Experimental Study of Supersonic combustion of Hydrogen in a Vitiated Airstream," NASA TM X-2828, September 1973.

[25] Sandia National Laboratories, TNF Workshop website. http://www.ca.sandia.gov/TNF/ (2005).

[26] University of Sydney, Thermal Research Group website, Bluff-Body Flames. http://www.mech.eng.usyd.edu.au/thermofluids/bluff.htm (2005).

[27] Barlow, R. S. and Frank, J. I., Effects of turbulence on species mass fractions in methane/air jet flames. *Proc. Combust. Inst.* **27** (1998) 1087–1095.

[28] Bilger, R. W., Pope, S. B., Bray, K. N. C. and Driscoll, J. F., Paradigms in turbulent combustion research. *Proc. Combust. Inst.* **30** (2005) 21–42.

[29] Colucci, P. J., Jaberi, F. A., Givi, P. and Pope, S. B., Filtered density function for large eddy simulation of turbulent reacting flows. *Phys. Fluids* **10**(2) (1998) 499–515.

[30] Drozda, T. G., *Large Eddy Simulation of a Piloted Diffusion Flame (Sandia Flame D) and a Bluff-Body Flame (Sydney Flame).* Ph.D. Thesis, Department of Mechanical Engineering, University of Pittsburgh, Pittsburgh, PA (2005).

[31] Gicquel, L. Y. M., Givi, P., Jaberi, F. A. and Pope, S. B., Velocity filtered density function for large eddy simulation of turbulent flows. *Phys. Fluids* **14**(3) (2002) 1196–1213.

[32] Givi, P., Filtered density function for subgrid scale modeling of turbulent combustion. *AIAA J.* **44**(1) (2006) 16–23.

[33] Jaberi, F. A., Colucci, P. J., James, S., Givi, P. and Pope, S. B., Filtered mass density function for large eddy simulation of turbulent reacting flows. *J. Fluid Mech.* **401** (1999) 85–121.

[34] Janicka, J. and Sadiki, A., Large eddy simulation of turbulent combustion systems. *Proc. Combust. Inst.* **30** (2005) 537–547.

[35] Masri, A. R., Dibble, R. W. and Barlow, R. S., The structure of turbulent nonpremixed flames revealed by Raman-Rayleigh-LIF measurements. *Prog. Energy Combust. Sci.* **22** (1996) 307–362.

[36] Mungal, M. G. and Dimotakis, P. E., Mixing and combustion with low heat release in a turbulent mixing layer. *J. Fluid Mech.* **148** (1984) 349–382.

[37] Nooren, P. A., Versiuis, M., Van der Meer, T. H., Barlow, R. S. and Frank, J. H., Raman-Rayleigh-LIF measurements of temperature and species concentrations in the Delft piloted turbulent jet diffusion flame. *Applied Physics* **B71** (2000) 95–111.

[38] Pope, S. B., *Turbulent Flows*. Cambridge, UK: Cambridge University Press (2000).

[39] Sheikhi, M. R. H., *Joint Velocity-Scalar Filtered Density Function for Large Eddy Simulation of Turbulent Reacting Flows*. Ph.D. Thesis, Department of Mechanical Engineering, University of Pittsburgh, Pittsburgh, PA (2005).

[40] Sheikhi, M. R. H., Drozda, T. G., Givi, P., Jaberi, F. A. and Pope, S. B., Large eddy simulation of a turbulent nonpremixed piloted methane jet flame (Sandia Flame D). *Proc. Combust. Inst.* **30** (2005) 549–556.

[41] Sheikhi, M. R. H., Drozda, T. G., Givi, P. and Pope, S. B., Velocity-scalar filtered density function for large eddy simulation of turbulent flows. *Phys. Fluids* **15**(8) (2003) 2321–2337.

[42] Qin, Z., Lissianski, V., Yang, H., Gardiner, W.C.Jr., Davis, S.G., and Wang, H., Proc. Combust. Inst., 28:1663-1669 (2000).

[43] Singh, D. J. and Jachimowski, C. J., Quasiglobal Reaction Model for Ethylene Combustion, *AIAA J.*, **32** (1):213-216 (1993).

[44] Wang, W. and Rogg, B., "Premixed Ethylene/Air and Ethane/Air Flames: Reduced Mechanisms Based on Inner Iterations," in *Reduced Kinetic Mechanisms for Applications in Combustion Systems*, Peters, N. and Rogg, B., editors, Lecture Notes in Physics, Vol. M15, Springer Verlag, 1993.

[45] Chelliah, H.K. and Thaker, A.A., "Reduced Reaction Models for Ethylene Ignition and Oxidation," 37th AIAA Aerospace Sciences Meeting and Exhibit, Reno, NV, January, 1999.

[46] Peters, N., in "Numerical Simulation of Combustion Phenomena" (R. Glowinski, B. Larrouturou, and T. Temam, eds.), Lecture Notes in Physics, Springer-Verlag, Vol. 214:90 (1985).

[47] Lam, H., "Singular Perturbation for Stiff Equations Using Numerical Methods," in *Recent Advances in the Aerospace Sciences* (C. Casci, Editor), Plenum Press, New York, 1985, pp. 3-20.

[48] Chen J.Y. "A general procedure for constructing reduced reaction *Combust. Sci. and Tech.* **57**:89-94 (1988).

[49] Maas, U. and Pope, S.B. *Combust. and Flame* "Simplifying Chemical Kinetics: Intrinsic Low-Dimensional Manifolds in Composition Space," **88**(3-4):239-264 (1992).

[50] Zambon, A.C. and Chelliah, H.K., "Explicit Reduced Reaction Models for C2H4-, CH4-, and H2-Air Mixtures," to be submitted to *Combust. and Flame.*